Hall Current and Ion-Slip Effects on the Entropy Generation of Couple Stress Fluid with Velocity Slip and Temperature Jump

A.A. Opanuga*, O.O. Agboola, H. I. Okagbue, A.M. Olanrewaju

Abstract**—** In this work, analytical study of Hall current and Ion-slip effects on the rate of entropy generation of couple stress fluid is considered. The obtained partial differential equations governing the flow are reduced to ordinary differential equations by similarity variables, semi-analytical solution of the dimensionless nonlinear coupled differential equations for velocity, temperature, entropy generation and Bejan number are constructed using Differential Transform Technique. Effects of Hall current, Ion-slip, couples stress and magnetic parameters are presented and discussed graphically. From the results it is observed that Hall current and rotation parameters enhance secondary velocity, fluid temperature and entropy generation. In addition rarefaction and Hartman number reduce fluid temperature and entropy generation.

Keywords**—**Velocity Slip, Temperature Jump, Hall Current, Ion-slip, Entropy Generation, Couple Stress Fluid, Differential Transform Method

I. Introduction

Recently, the study of Microfluidics has become an important area of research due to its wide applications in various fields such as physical, biological, chemical, engineering, medical etc. This has resulted in various theoretical and experimental study of flow through a channel of microscale size. Investigation of the flow of fluid through microchannels is determined by the Knudsen number, Kn. The Knudsen number is the ratio of the molecular mean free path (λ) to characteristic length, i.e. $Kn = \lambda / H$ For the flow within the range of 0.001 < Kn < 0.1, the standard Navier–Stokes with slip boundary conditions are applicable [1].

Several investigations have been undertaken to determine the effect of velocity slip and temperature jump on macrochannel system. Hooman [2] considered the effects of velocity slip, temperature jump, viscous dissipation, and duct geometry on the irreversibility analysis of microscale forced convection flow. It was submitted that the obtained results can be generalized to the macroscale flow when $Kn = 0$. Khadrawi and Al-Shyyab [3] analysed the effects of slip velocity and temperature jump on heat and fluid flowing axially in micro-concentric cylinders. Chen and Tian [4] applied lattice Boltzmann numerical technique to investigate the fluid flow and heat transfer between two horizontal parallel plates with velocity slip and temperature jump. Zhenga et al. [5] presented velocity slip and temperature jump effects on MHD flow and heat transfer over a porous shrinking surface. Adesanya [6] studied free convective flow of heat generating fluid with velocity slip and temperature jump. In the work it was concluded that an increase in the slip parameter enhanced flow velocity while fluid temperature is enhanced by temperature jump parameter. Other studies on this subject are found in Refs. [7-12].

In recent years, attention has been devoted to natural convection flow with heat transfer. Since then extensions have been conducted to include several other phenomena such as the effects of magnetic fields for electrically conducting fluid, [13-19]. All these investigators assumed small and moderate value of magnetic field resulting in unnoticeable impact in the flow, however current application of magnetohydrodynamics is geared towards strong magnetic fields due to its significance in magnetic fusion systems, electrically-conducting aerodynamics, energy generators, Hall accelerators and flight magnetohydrodynamics. Moreover, investigations have shown the significance of the interaction between Coriolis and electromagnetic forces in MHD flows. It is noteworthy that Coriolis and MHD forces are comparable in magnitude, and Coriolis force induces secondary flow in the fluid. Rotating MHD flows have important applications in the turbo machinery, solidification process in metallurgy and some astrophysical problems.

Nanda and Mohanty [20] considered magnetohydrodynamic flow in a rotating channel. Jana et al. [21] studied the MHD Couette flow and heat transfer with rotation effect. Effects of Hall current on hydromagnetic rotating Couette flow was investigated by Ghosh [22].

This work was supported by Covenant University Centre for Research, Innovation and Development, Ota, Nigeria.

A. A. Opanuga, O.O. Agboola, H.I. Okagbue, and S.A. Olanrewaju are with the Department of Mathematics, Covenant University, Ota, Nigeria.
(e-mail:abiodun.opanuga@covenantuniversity.edu.ng,, hilary.okagbue@covenantuniversity.edu.ng ola.agboola@covenantuniversity.edu.ng, anuoluwapo oluwlanrewaju).

Unsteady MHD Couette flow in a rotating system was analysed by Seth et al. [23]. Rao and Rao [24] examined the MHD flow of Rivlin–Ericksen fluid of rotating second grade contained between two infinite parallel. Recently, investigations on Hall current and Ion slip effects have been conducted by Sandeep [25], Reddya et al. [26], Kumar et al. [27] and Opanuga et al. [28-29].

In this article, the objective is the application of first and second laws of thermodynamics in the analysis of the influence of velocity slip, temperature jump, Hall current and rotation parameters on the flow of couple stress fluid. In literature, several investigations regarding the factors responsible for entropy generation have been reported, see Refs. [30-34]. Couple stress fluid irreversibility due to the effects of Hall current, Ion slip, velocity slip and temperature jump have not been accorded the required attention in spite of its wide application, hence this study addresses the noticed gap.

In this analysis, Zhou method [35] is used to obtain the solution of the velocity and temperature profiles due to its simplicity and rapid convergence to the exact, where it exists. This technique has been widely applied to solve various linear and nonlinear models by several authors [36-40].

II. Problem Formulation

Consider the fully developed steady flow of viscous, incompressible couple stress fluid in a micro-porous-channel in the presence of transverse magnetic field. A Cartesian coordinate system is taken such that the x-axis is along the lower plate in the flow direction while the y-axis is perpendicular to the channel plates. The plates are heated asymmetrically with the cooler one $(y=-h)$ maintained at a temperature T_1 while the hotter plate $(y=+h)$ is at temperature T_2 where $(T_2 > T_1)$. In addition, assumption of relatively high electron-atom collision frequency is taken so that the influence of Hall current and ion slip are upheld. The fluid is rotating with an angular velocity Ω^* about the normal to the plate. The governing equations for the continuity, momentum and energy are [41]:

$$\frac{\partial v}{\partial y}=0 \tag{1}$$

$$\rho\nu_0\frac{\partial u}{\partial y}+2\Omega^* w=\mu\frac{\partial^2 u}{\partial y^2}-\eta^*\frac{\partial^4 u}{\partial y^4} -\frac{\sigma B_0^2}{1+m^2}(u-mw); \tag{2}$$

$$\rho\nu_0\frac{\partial w}{\partial y}-2\Omega u=\mu\frac{\partial^2 w}{\partial y^2}-\eta^*\frac{\partial^4 w}{\partial y^4}- \frac{\sigma B_0^2}{1+m^2}(w+mu); \tag{3}$$

$$\rho c_p v_0\frac{\partial T}{\partial y}=k\frac{\partial^2 T}{\partial y^2}+\mu\left[\left(\frac{\partial u}{\partial y}\right)^2+\left(\frac{\partial w}{\partial y}\right)^2\right]+ \eta^*\left[\left(\frac{\partial^2 u}{\partial y^2}\right)^2+\left(\frac{\partial^2 w}{\partial y^2}\right)^2\right]+\frac{\sigma B_0^2}{1+m^2}\left(u^2+w^2\right) \tag{4}$$

The appropriate boundary conditions for the velocity slip and temperature jump at the fluid–wall interface [42-43] are given as

$$u=\beta_v kn\frac{\partial u}{\partial y}, w=\beta_v kn\frac{\partial w}{\partial y}, \theta=\xi+\beta_t kn\frac{\partial T}{\partial y}, \quad y=-h \tag{5}$$

$$\frac{\partial^2 u}{\partial y^2}=0, \frac{\partial^2 w}{\partial y^2}=0, \theta=1-\beta_t kn\frac{\partial T}{\partial y}, y=+h$$

Using these transformation variables

$$y=\eta h, u=\frac{\nu}{h}f, w=\frac{\nu}{h}g, \theta\left(T_2-T_0\right)=T-T_0 \tag{6}$$

equations (1-4) yield the following dimensionless form;

$$a^2 f^{(iv)}-f''+\mathrm{Re}\, f'+2K^2 g+ \frac{H^2}{1+m^2}(f+mg)=0, \tag{7}$$

$$a^2 g^{(iv)}-g''+\mathrm{Re}\, g'-2K^2 f- \frac{H^2}{1+m^2}(mf-g)=0 \tag{8}$$

$$\theta''-\mathrm{Re}\,\mathrm{Pr}\,\theta'+Br\left[\left(f'\right)^2+\left(g'\right)^2\right]+ a^2 Br\left[\left(f''\right)^2+\left(g''\right)^2\right]+\frac{BrH^2}{1+m^2}\left(f^2+g^2\right)=0 \tag{9}$$

and the dimensionless boundary conditions are

$$f=\beta_v knf', g=\beta_v kng', \theta=\xi+\beta_t kn\theta', y=-1; \quad f''=g''=0, \theta=1-\beta_t kn\theta', y=1 \tag{10}$$

In Equations (7-10), primes denote the derivatives with respect to η

$$a^2=\frac{\eta^*}{h^2\mu},Br=\frac{\mu v^2}{kh^2\left(T_2-T_0\right)},\Pr=\frac{\mu C_p}{k},$$
$$H^2=\frac{\sigma B_0^2h^2}{\mu},\mathrm{Re}=\frac{\rho v_0h}{\mu},K^2=\frac{\Omega^*h^2}{\mu},$$
$$\Omega=\frac{T_2-T_0}{T_0},\xi\left(T_2-T_0\right)=T_1-T_0, \quad (11)$$
$$\beta_v=\frac{2-F_v}{F_v},\beta_t=\frac{2-F_v}{F_v}\frac{2\gamma_s}{\gamma_s+1}\frac{1}{\Pr},\gamma_s=\frac{c_p}{c_v},$$
$$kn=\frac{\lambda}{h},\ln=\frac{\beta_t}{\beta_v},Ns=\frac{E_GT_0h^2}{k\left(T_2-T_0\right)}$$

III. DIFFERENTIAL TRANSFORMATION METHOD OF SOLUTION

The basic operations and properties of differential transform method, which are relevant to the problem solved in this paper are summarized in the table that follows:

Table 1: Operations and Properties of Differential Transform Method

Original function	Transformed function
$f(y)=u(y)\pm w(y)$	$F(k)=U(k)\pm W(k)$
$f(y)=\frac{d^nu(y)}{dy^n}$	$F(k)=\frac{(k+n)!}{k!}U(k+n)$
$f(y)=u^2$	$F(k)=\sum_{r=0}^{k}U(r)U(k-r)$
$f(y)=\left(\frac{du(y)}{dy}\right)^2$	$F(k)=\sum_{r=0}^{k}(r+1)(k-r+1)U(r+1)U(k-r+1)$
$f(y)=\left(\frac{d^2u(y)}{dy^2}\right)^2$	$F(k)=\sum_{r=0}^{k}(r+1)(r+2)(k-r+1)(k-r+2)U(r+2)U(k-r+2)$

To apply Differential Transform Method (DTM) to the problem in view, the basic properties of DTM which are outlined in Table 1, are invoked appropriately on equations (7)-(9). Doing this, one obtains the following recurrence relations:

$$F(k+4)=\frac{1}{a^2(k+4)!}\left[\begin{array}{l}(k+1)(k+2)F(k+2)-\\ \mathrm{Re}(k+1)F(k+1)-2K^2G(k)\\ -\frac{H^2}{1+m^2}\left(F(k)+G(k)\right)\end{array}\right] \quad (12)$$

$$G(k+4)=\frac{1}{a^2(k+4)!}\left[\begin{array}{l}(k+1)(k+2)G(k+2)-\\ \mathrm{Re}(k+1)G(k+1)+2K^2F(k)\\ +\frac{H^2}{1+m^2}\left(F(k)+G(k)\right)\end{array}\right] \quad (13)$$

$$\Theta(k+2)=\frac{1}{(k+2)!}\left[\mathrm{Re}\Pr(k+1)\Theta(k+1)+\right.$$
$$Br\left(\sum_{r=0}^{k}(r+1)F(r+1)(k-r+1)F(k-r+1)\right.$$
$$\left.+\sum_{r=0}^{k}(r+1)G(r+1)(k-r+1)G(k-r+1)\right)$$
$$-a^2Br\left(\sum_{r=0}^{k}\frac{(r+1)(r+2)F(r+2)(k-r+1)}{(k-r+2)F(k-r+2)}\right) \quad (14)$$
$$+a^2Br\left(\sum_{r=0}^{0}\frac{(r+1)(r+2)G(r+2)(k-r+1)}{(k-r+2)G(k-r+2)}\right)$$
$$\left.-\frac{BrH^2}{1+m^2}\left(\sum_{r=0}^{k}F(r)F(k-r)+\sum_{r=0}^{k}G(r)G(k-r)\right)\right]$$

where $F(k)$, $G(k)$ and $\Theta(k)$ are the transformed functions of $f(y)$, $g(y)$ and $\theta(y)$ respectively. These are given by

$$f(y)=\sum_{k=0}^{\infty}y^kF(k),\quad G(y)=\sum_{k=0}^{\infty}y^kG(k),$$
$$\theta(y)=\sum_{k=0}^{\infty}y^k\Theta(k) \quad (15)$$

We choose the following initial conditions:

$$F(0)=a_1,\quad F(1)=a_2,\quad F(2)=a_3,\quad F(3)=a_4,$$
$$G(0)=a_5,\quad G(1)=a_6,\quad G(2)=a_7,\quad G(3)=a_8, \quad (16)$$
$$\Theta(0)=a_9,\quad \Theta(1)=a_{10}$$

By substituting equations (15) into equations (12)-(14), we can determine the values of $F(k)$, $G(k)$ and $\Theta(k)$ for $k=0,1,\ldots,$ recursively. The values of $F(k)$, $G(k)$ and $\Theta(k)$ for $k=0,1,\ldots,$ are now substituted back into equations (15) to obtain the series solutions in the form:

$$f(y)=\sum_{k=0}^{n}y^kF(k),\quad G(y)=\sum_{k=0}^{n}y^kG(k),$$
$$\theta(y)=\sum_{k=0}^{n}y^k\Theta(k) \quad (17)$$

Where the value of n is determined by convergence.

We next invoke the transformed form of boundary conditions on (17) to determine the values of all the unknown coefficients stated in (16). Taking the values of the parameters Coding equations (12-16) in symbolic Maple software yields the approximate solution. The results are presented in Figures 1-4.

A. Entropy Generation Analysis

The local entropy generation expression for the flow is given as, Bejan [44]

$$E_G = \frac{k}{T_0^2}\left(\frac{\partial T}{\partial y}\right)^2 + \frac{\mu}{T_0}\left(\left(\frac{\partial u}{\partial y}\right)^2 + \left(\frac{\partial w}{\partial y}\right)^2\right) + \frac{\eta^*}{T_0}\left(\left(\frac{\partial^2 u}{\partial y^2}\right)^2 + \left(\frac{\partial^2 w}{\partial y^2}\right)^2\right) + \frac{\sigma B_0^2}{T_0}\left(w^2 + u^2\right), \quad (18)$$

$$Ns = \theta'^2(\eta) + \frac{Br}{\Omega}\left[\left(f'(\eta)\right)^2 + \left(g'(\eta)\right)^2 + a^2\left(\left(f''(\eta)\right)^2 + \left(g''(\eta)\right)^2\right) + H^2\left(f^2(\eta) + g^2(\eta)\right)\right] \quad (19)$$

$$N_1 = \theta'^2(\eta), N_2 = \frac{Br}{\Omega}\left[\left(f'(\eta)\right)^2 + \left(g'(\eta)\right)^2 + a^2\left(\left(f''(\eta)\right)^2 + \left(g''(\eta)\right)^2\right) + H^2\left(f^2(\eta) + g^2(\eta)\right)\right] \quad (20)$$

The Bejan number can be written as

$$Be = \frac{N_1}{N_s} = \frac{1}{1+\Phi}, \quad \Phi = \frac{N_2}{N_1}. \quad (21)$$

In equation (21), Bejan number ranges from 0 to 1. Note that $Be = 0$ represents the limit at which fluid friction irreversibility dominates entropy generation, while $Be = 1$ corresponds to the dominance of heat transfer irreversibility over fluid friction irreversibility and $Be = 0.5$ is the case when heat transfer and fluid friction entropy generation rates are equal.

IV. RESULTS AND DISCUSSION

In this present work, analysis of Hall current and ion-slip effects on the rate of entropy generation of couple stress fluid through a microchannel in the presence of an induced magnetic field is governed by some thermophysical parameters such as Hall current parameter (m), rotation parameter (K^2), rarefaction $(\beta_v kn)$, wall-ambient temperature difference ratio (WTDR) (ξ) and Hartmann number (H). The influence of the parameters at different values on fluid velocity $(f(\eta), g(\eta))$, temperature profile $\theta(\eta)$, entropy generation expression (Ns) and Bejan number (Be) are presented in Figures 1-4 by fixing the parameters

$Br = 0.5, \Pr = 0.71, a = 2, \mathrm{Re} = 2, \beta_v kn = 0.05,$
$\ln = 1.667, \Omega = 1$.

Figures 1A and 1B represent the influence of Hall current on fluid velocity $(f(\eta), g(\eta))$. It is clear that primary velocity $(f(\eta))$ reduces as Hall parameter increases whereas secondary velocity $(g(\eta))$ increases. This observation reveals that Hall current tends to speed-up secondary fluid velocity, which agrees with the fact that the presence of Hall parameter (m) suppresses the resistive influence of the magnetic field. Figures 1C and 1D depict the effect of rotation parameter (K^2) on fluid velocity. It is noticed that primary fluid velocity $(f(\eta))$ decelerates while secondary fluid motion $(f(\eta))$ accelerates with rising values of (K^2). This is consistent with the known fact that rotation accelerates secondary flow while inhibiting primary flow field. This accelerating impact of rotation is only dominant in the region close to the plate whereas it has a reverse effect on secondary fluid velocity in the region away from the plate. Coriolis effect is attributed to this phenomenon.

In Figure 1E it is noticed that fluid velocity reduces but rises in Figure 1F as rarefaction parameter increases. The observed increase in the motion of fluid in Figure 1F is linked to the rising values of Knudsen number (kn) which tends to enhance fluid velocity as a result of the reduction in fluid-wall interaction. Effect of Harman number on fluid velocity is depicted in Figures 1G and 1H. It shows that fluid motion is accelerated in Fig. 1G while it reduces in Fig. 1H. This is known to have resulted from the Lorentz force which usually inhibits fluid motion in electrically conducting fluid.

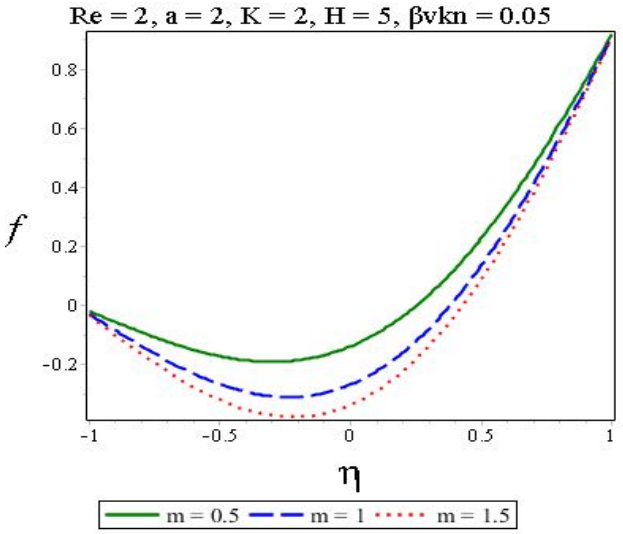

Fig 1A: Primary velocity for different m

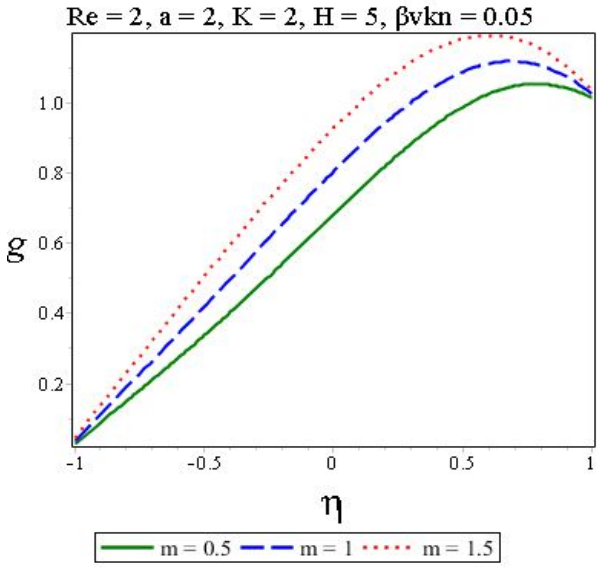

Fig 1B: Secondary velocity for different m

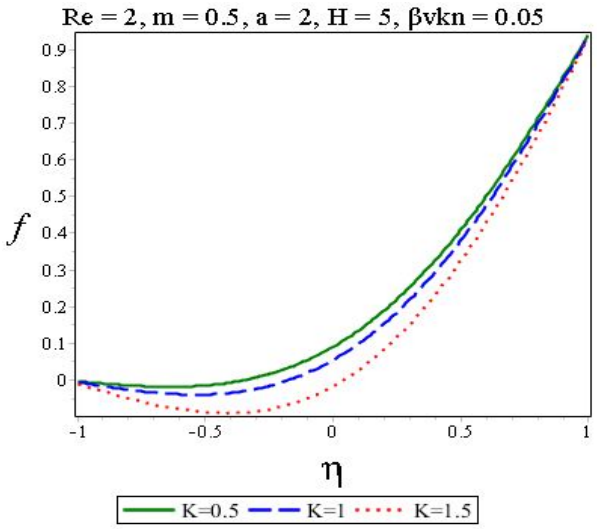

Fig 1C: Primary velocity for different K

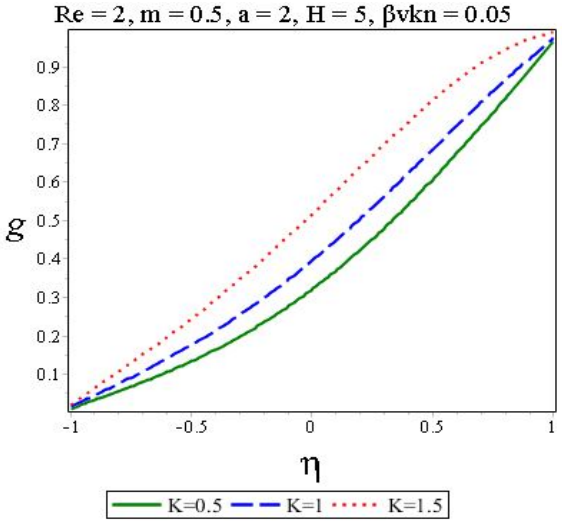

Fig 1D: Secondary velocity for different K

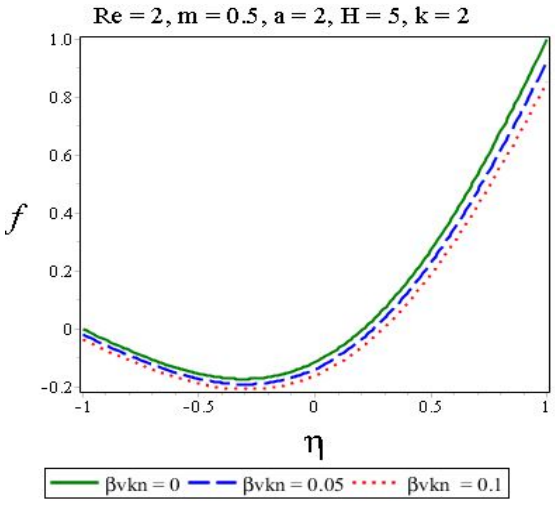

Fig 1E: Primary velocity for different $\beta_v kn$

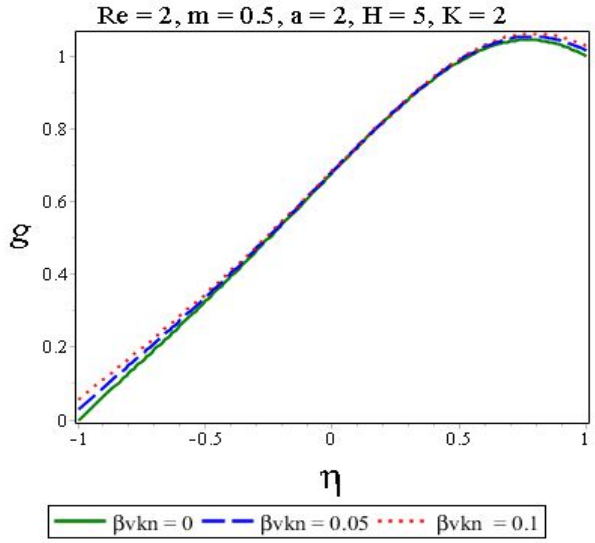

Fig 1F: Secondary velocity for different $\beta_v kn$

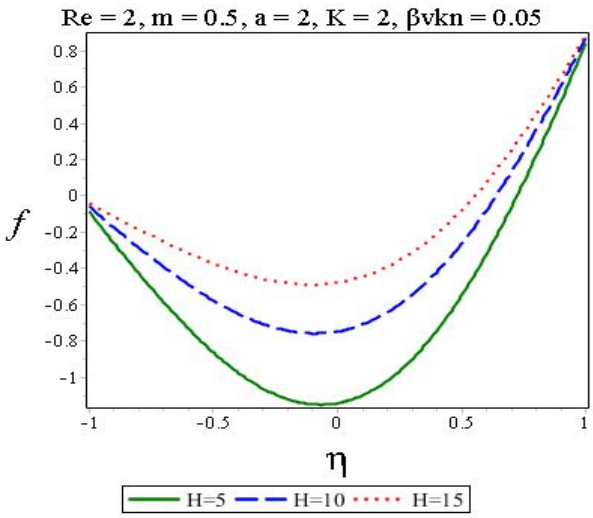

Fig 1G: Primary velocity for different H

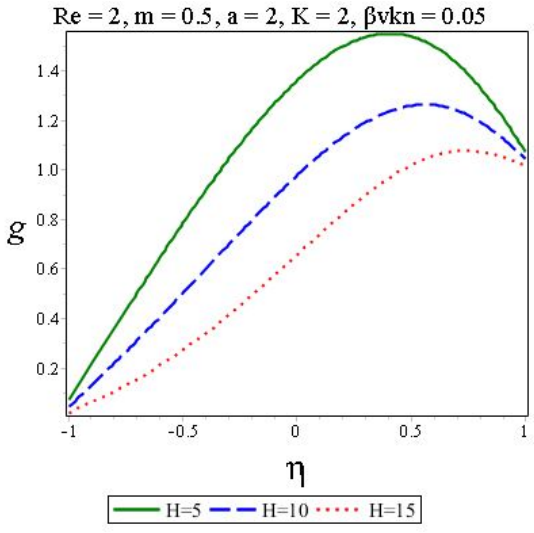

Fig 1H: Secondary velocity for different H

In Figure 2A and 2B, effects of Hall current and rotation parameters on fluid temperature are presented. It is evident that temperature profile is enhanced as Hall and rotation parameters increase. As submitted above the inclusion of Hall current parameter (m) in the flow has a significant impact on fluid temperature because magnetic effect is subdued. In Figures 2C and 2D, rarefaction and magetic field effects on fluid temperature are represented. Fluid temperature is raised in Figure 2C whereas it is depreciates in Figure 2D. The increase registered in Figure 2C is due to a rise Knudsen number (Kn), which increases rarefaction and hence fluid-wall interaction decreases. It is interesting to observe that fluid temperature increases significantly in Figure 2E as wall-ambient temperature difference ratio increases.

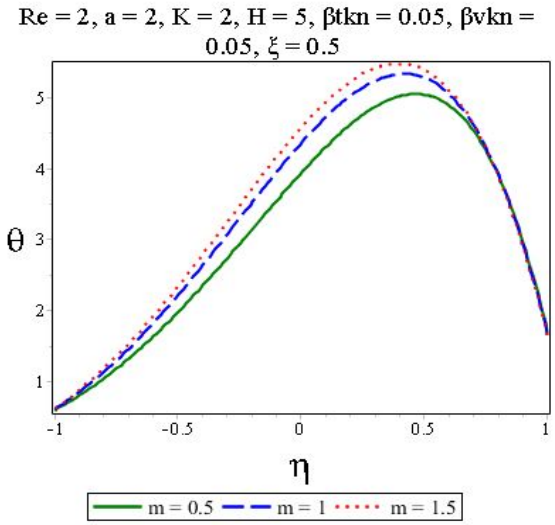

Fig 2A: Hall current for different $\theta(\eta)$

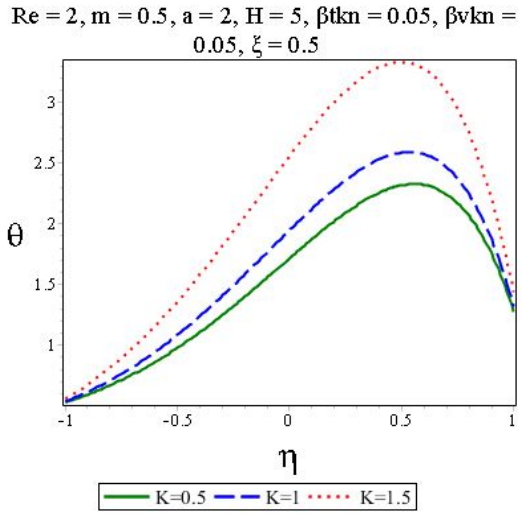

Fig 2B: Rotation parameter for different $\theta(\eta)$

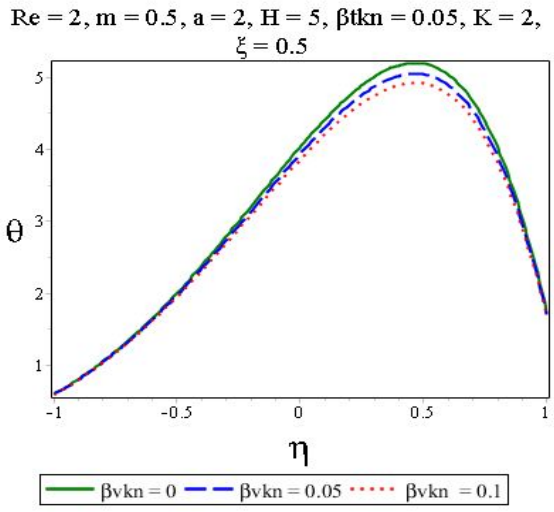

Fig 2C: Rarefaction for different $\theta(\eta)$

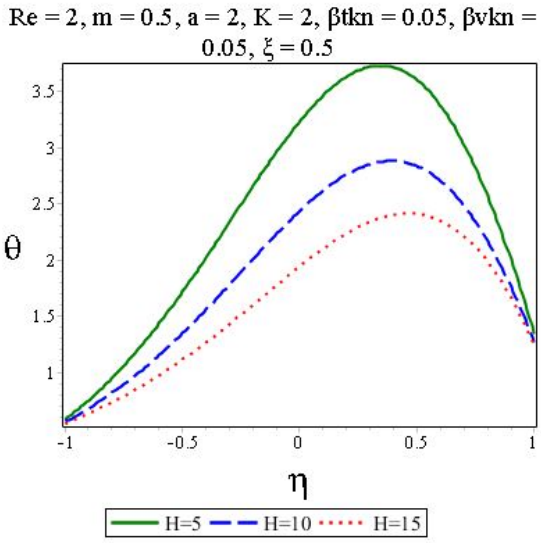

Fig 2D: Magnetic field for different $\theta(\eta)$

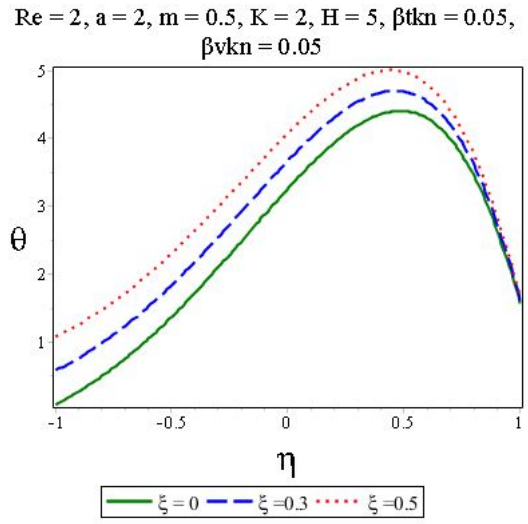

Fig 2E: WTDR for different $\theta(\eta)$

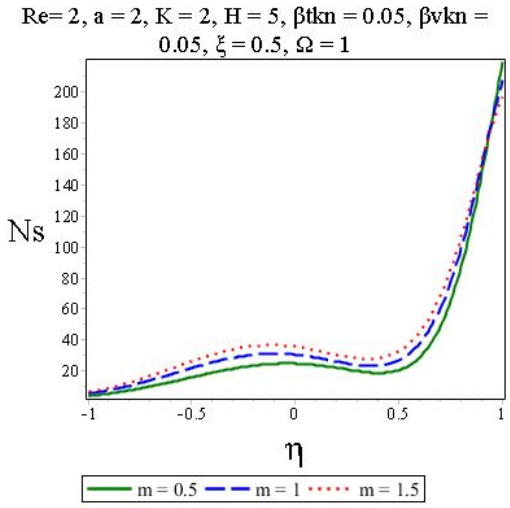

Fig 3A: Hall current for different *Ns*

Next is the response of entropy generation to variation in fluid parameters. In Figure 3A and 3B entropy generation rises higher as Hall current and rotation parameter increase. This is expected since increase in these parameters raise fluid temperature as depicted in Figures 2A and 2B. This increase resulted in the disorderliness of fluid particles leading to entropy production. On the other hand fluid entropy generation is lowered in Figures 3C and 3D as rarefaction and Magnetic field parameters increase. Generally, Hartmann number has the effect to suppress fluid velocity (see Figure 1C) and then to reduce fluid temperature (see Figure 2D). The total effect of this is that major part of the fluid becomes practically motionless hence the reduction in entropy generation. In Figure 3E, increase in the values of wall-ambient temperature difference ratio (WTDR) (ξ) slightly reduce entropy generation in the region $-1 \le \xi \le 0.5$ while there is a rise in entropy generation around $0.6 \le \xi \le 1$

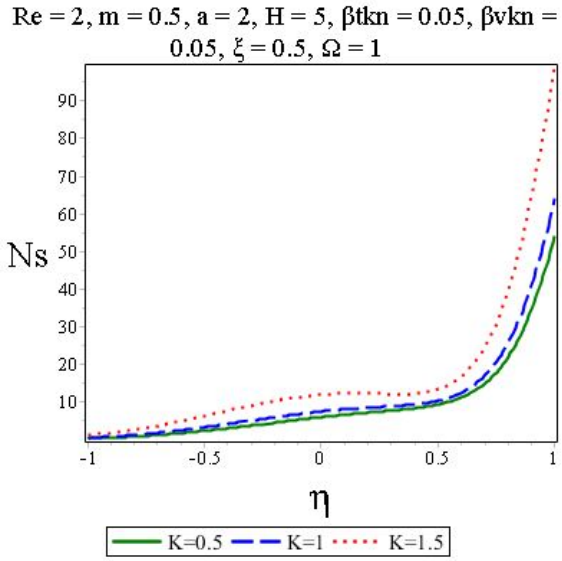

Fig 3B: Rotation parameter for different *Ns*

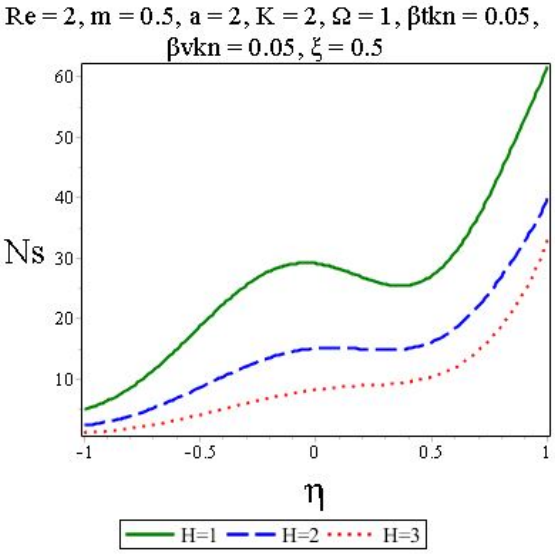

Fig 3D: Magnetic field for different *Ns*

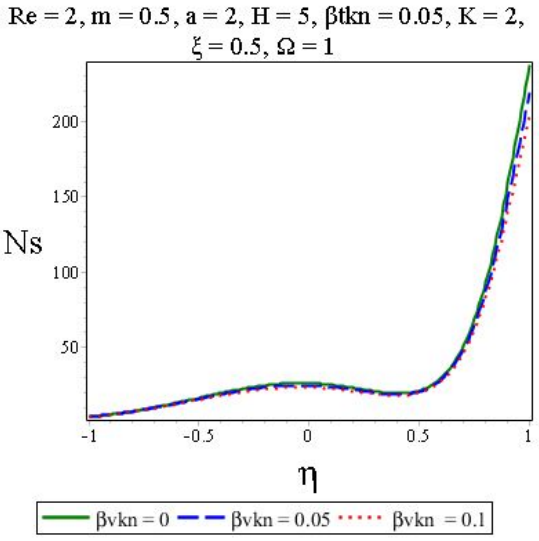

Fig 3C: Rarefaction for different *Ns*

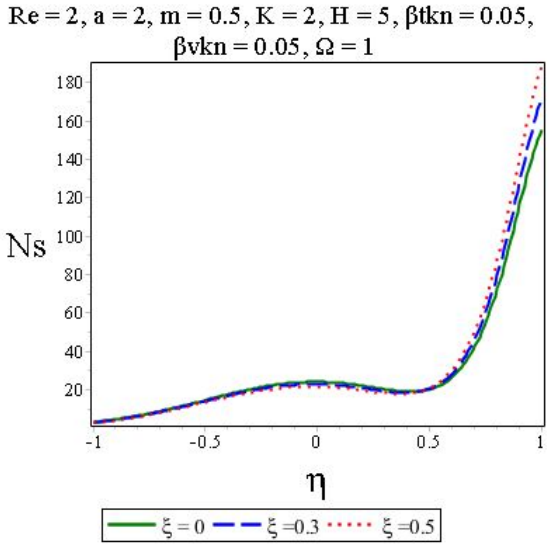

Fig 3E: WTDR for different *Ns*

Finally, Bejan number response to variation of the thermophysical parameters are displayed in Figures 4. In convective problem, entropy generation is being promoted by both heat transfer irreversibility (FTI) and fluid friction irreversibility (FFI). Equation (15) gives the expression for calculating fluid irreversibility, however the determination of the dominance of either FTI or FFI to total entropy generation is given by Bejan number in equation (18).

In Figures 4A, 4C and 4E Bejan number reduces at both the wall $\eta = -1$ and middle of the microchannel but rises at the microchannel wall $\eta = 1$ with increase in Hall paremeter, rarefaction parameter and wall-ambient temperature difference ratio. A reverse phenomenon is noticed in Figures 4B and 4D as rotation and magnetic parameters are varied. The submissions above reveal that both heat transfer and fluid friction contribute to entropy generation.

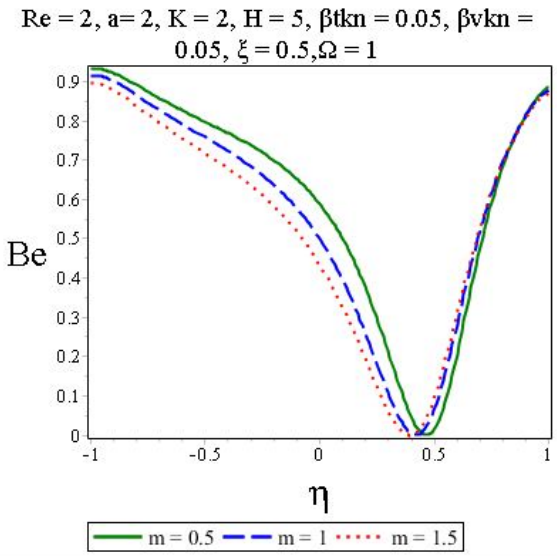

Fig 4A: Hall current for different *Be*

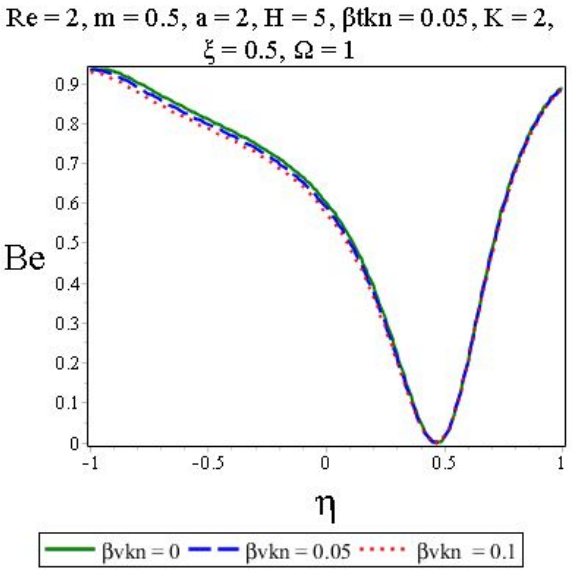

Fig 4C: Rarefaction for different *Be*

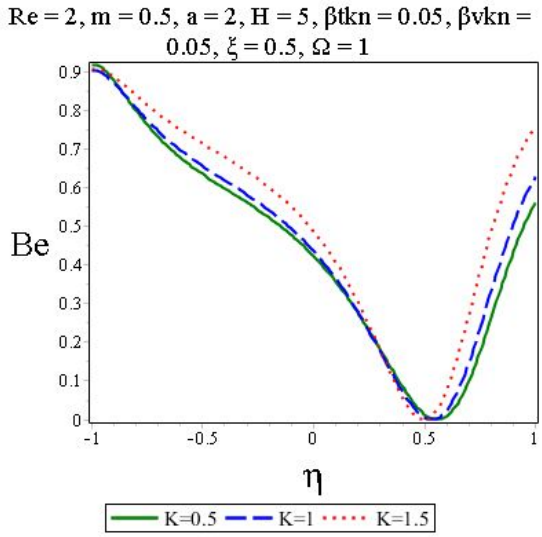

Fig 4B: Rotation parameter for different *Be*

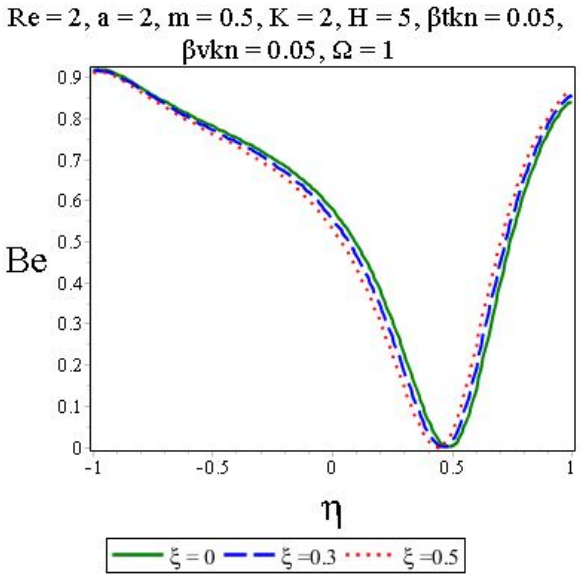

Fig 4E: WTDR for different *Be*

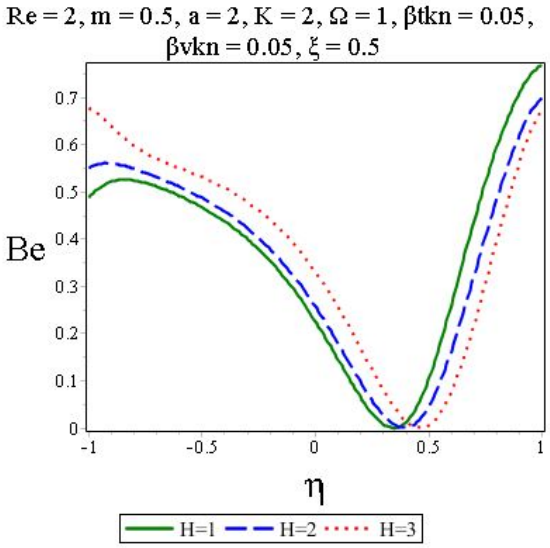

Fig 4D: Magnetic field for different *Be*

Conclusions

In this article, a mathematical model for the flow of couple stress fluid through a microchannel has been developed to study the influence of the irreversibility associatied with Hall current and Ion-slip. Velocity slip and temperature jump boundary conditions are included in the model and the velocity and temperature profiles are solved by differential transform method, the results are used to determine the entropy generation and Bejan number. Results show that Hall current and rotation parameter increase entropy generation whereas entropy generation is suppressed by rarefaction parameter and Hartman number. Furthermore it is shown that both fluid friction and heat transfer contributed to entropy generation.

References

[1] Renksizbulut, M., Niazmand, H. and Tercan, G. Slip-flow and heat transfer in rectangular microchannels with constant wall temperature, International Journal of Thermal Sciences. 45, 2006, pp. 870–881.

[2] Hooman, K. Entropy generation for microscale forced convection: effects of different thermal boundary conditions, velocity slip, temperature jump, viscous dissipation, and duct geometry, International Communications in Heat and Mass Transfer, 34, 2007, pp. 945–957.

[3] Khadrawi, A.F. and Al-Shyyab, A. Slip flow and heat transfer in axially moving micro-concentric cylinders International Communications in Heat and Mass Transfer, 37, 2010, pp.1149–1152, http://dx.doi.org/10.1016/j.icheatmasstransfer.2010.06.006.

[4] Chen, S. and Tian, Z. Simulation of thermal micro-flow using lattice Boltzmann method with Langmuir slip model International Journal of Heat and Fluid Flow, 31, 2010, pp. 227–235, http://dx.doi.org/10.1016/j.ijheatfluidflow.2009.12.006.

[5] Zhenga, L., Niua, J., Zhangb, X. and Gaoc, Y. MHD flow and heat transfer over a porous shrinking surface with velocity slip and temperature jump, Mathematical and Computer Modelling, 56, 2012, pp. 133–144.

[6] Adesanya, S.O. Free convective flow of heat generating fluid through a porous vertical channel with velocity slip and temperature jump, Ain Shams Engineering Journal, 2015, http://dx.doi.org/10.1016/j.asej.2014.12.008

[7] Aziz, A. and Niedbalski, N. Thermally developing microtube gas flow with axial conduction and viscous dissipation, International Journal of Thermal Sciences, 50, 2011, pp. 332–340, http://dx.doi.org/10.1016/j.ijthermalsci.2010.08.003.

[8] Malvandi, A. and Ganji, D.D. Mixed convective heat transfer of water/alumina nanofluid inside a vertical microchannel, Powder Technology, 263, 2014, pp. 37–44, http://dx.doi.org/10.1016/j.powtec.2014.04.084.

[9] Jha, B.K. and Aina, B. Mathematical modelling and exact solution of steady fully developed mixed convection flow in a vertical micro-porous-annulus, Afrika Matematika, 26 2015, pp. 1199–1213, http://dx.doi.org/10.1007/s13370-014-0277-4.

[10] Rostami, A.A., Saniel N. and Mujumdar, A.S. Flow and heat transfer for gas flowing in microchannels: a review. Heat and Mass Transfer, 38(4-5), 2002, pp. 359–367.

[11] Guo, Z.Y. and Li, Z.X. Size effect on microscale single phase flow and heat transfer, International Journal of Heat and Mass Transfer, 46(1), 2003, pp. 149-159.

[12] Morini, G.L. Single phase convective heat transfer in microchannel: a review of experimental results, International Journal of Thermal Sciences, 43, 2004, pp. 631–651.

[13] Gbadeyan, J.A. and Idowu, A.S. Radiation effect of magnetohydrodynamic flow of gas between concentric spheres, Journal of the Nigerian Association of Mathematical Physics, 10 (2006): 305-314

[14] Adesanya, S.O. and Makinde, O.D. Heat Transfer to Magnetohydrodynamic Non-Newtonian Couple Stress Pulsatile Flow Between two Parallel Porous Plates, Zeitschrift für Naturforschung. 67a, 2012, pp. 647 – 656.

[15] Mutuku-Njane, W.N. and Makinde, O.D. Combined effects of buoyancy force and Navier slip on MHD flow of a Nanofluid over a convectively heated vertical porous plate, The Scientific World Journal, 2013, 8 pages, http://dx.doi.org/10.1155/2013/725643

[16] Shehzad, S.A., Hayat, T. and Alsaedi, A. Influence of convective heat and mass conditions in MHD flow of nanofluid, Bulletin Of The Polish Academy Of Sciences Technical Sciences, 63(2), 2015), pp. 465-474.

[17] Adesanya, S.O., Oluwadare, J.A. Falade, J.A. and O.D. Makinde, Hydromagnetic natural convection flow between vertical parallel plates with time-periodic boundary conditions, Journal of Magnetism and Magnetic Materials, 396, 2015, pp. 295–303.

[18] Aydin, O. and Kaya, A. Radiation effect on MHD mixed convection flow about a permeable vertical plate, Heat and Mass Transfer, vol. 45(2), 2008, pp. 239–246.

[19] Adesanya, S.O., Falade, J.A. and Rach, R. Effect of couple stresses on hydromagnetic Eyring-Powell fluid flow through a porous channel, Theoretical and Applied Mechanics, 42(2), 2015, pp. 135–150.

[20] Nanda, R.S. and Mohanty, H.K. Hydromagnetic flow in a rotating channel, Applied Scientific Research. 24, 1970, pp. 65–78

[21] Jana, R.N., Datta, N. and Mazumder, B.S. Magnetohydrodynamic Couette flow and heat transfer in a rotating system, Journal of the Physical Society of Japan, 42, 1977, pp. 1034–1039.

[22] Ghosh, S.K. Effects of Hall current on MHD Couette flow in a rotating system with arbitrary magnetic field, Czechoslovak Journal of Physics, 52(1), 2002, pp. 51–63.

[23] Seth, G.S., Jana, R.N. and Maiti, M.K. Unsteady hydromagnetic Couette flow in a rotating system, International Journal of Engineering Science, 20, 1982, pp. 989–999.

[24] Rao A.R. and Rao, P.R. MHD flow of a second grade fluid in an orthogonal rheometer, International Journal of Engineering Science, 23(12), 1985, pp. 1387-1395

[25] Sandeep, N., Sugunamma, V. and Krishna, P.M. Aligned magnetic field, radiation and rotation effects on unsteady hydro magnetic free convection flow past an impulsively moving vertical plate in a porous medium. International Journal of Engineering Mathematics, 7, 2014. http://dx.doi.org/10.1155/2014/565162.

[26] Ramana Reddya, J.V., Sugunammaa, V., Sandeepb, N. and Sulochanab, C. Influence of chemical reaction, radiation and rotation on MHD nanofluid flow past a permeable flat plate in porous medium, Journal of the Nigerian Mathematical Society, 35, 2016, pp. 48–65.

[27] Kumar, D.A., Singh, K. and Sarveshanand, M. Effect of Hall current and wall conductance on hydromagnetic natural convective flow between vertical walls, Int. J. Industrial Mathematics, 9(4), 2017, pp. 289-299.

[28] Opanuga, A.A., Gbadeyan, J.A., Okagbue, H.I. and Agboola, O.O. Hall current and suction/injection effects on the entropy generation of third grade fluid, International Journal of Advanced and Applied Sciences, 5 (7), pp. 108-115.

[29] Opanuga, A.A., Okagbue, H.I. and Agboola, O.O. and Bishop, S.A. Second Law Analysis of Ion Slip Effect on MHD Couple Stress Fluid, International Journal of Mechanics, 12, pp. 96-101.

[30] Rashidi, M.M., Bhatti, M.M., Abbas, M.A. and Ali, M.E. Entropy generation on MHD blood flow of nanofluid due to peristaltic waves, Entropy, 18(117), 2016, doi:10.3390/e18040117
[31] Adesanya S.O. and Falade, J.A. Thermodynamics analysis of hydromagnetic third grade fluid flow through a channel filled with porous medium, Alexandria Engineering Journal, 54, 2015, pp. 615–622
[32] Opanuga, A.A., Gbadeyan, J.A., Agboola, O.O. and Okagbue, H.I. Effect of suction/injection on the entropy generation of third grade fluid with convective cooling, Defect and Diffusion Forum, 384, 2018, pp. 465-474.
[33] Opanuga, A.A., Gbadeyan, J.A. and Iyase,S.A. Second law analysis of hydromagnetic couple stress fluid embedded in a non-Darcian porous medium, IAENG International Journal of Applied Mathematics, 47(3), 2017, pp. 287-294.
[34] Opanuga, A.A., Okagbue, H.I., Agboola, O.O. and Imaga, O.F. Entropy generation analysis of buoyancy effect on hydromagnetic Poiseuille flow with internal heat generation, Defect and Diffusion Forum, 378, 2017, pp. 102-112.
[35] Zhou, J.K. Differential Transformation and its Applications for Electrical circuits, Huazhong University press, Wuhan, China, (1986).
[36] Biaza, J. and Eslami, M. Differential Transform method for Quadratic Riccati Differential Equation, International Journal of Nonlinear Science, 9(4), 2010, pp. 444-447.
[37] Agboola, O.O., Gbadeyan, J.A., Opanuga, A.A., Agarana, M.C., Bishop, S.A. and Oghonyon, J.G. Variational Iteration Method for Natural Frequencies of a Cantilever Beam with Special Attention to the Higher Modes, Proceedings of The World Congress on Engineering and Computer Science 2017, London, UK, July 5-7, 2017.
[38] Agboola, O.O., Opanuga, A.A. and Gbadeyan, J.A. Solution of third order ordinary differential equations using differential transform method, Global Journal of Pure and Applied Mathematics, 11(4), pp. 2511-2517.
[39] Opanuga, A.A. Edeki, S.O., Okagbue, H.I. and Akinlabi,G.O. A Novel approach for solving quadratic Riccati differential equations, International Journal of Applied Engineering Research, 10 (11), pp. 29121-29126.
[40] Opanuga, A.A., Edeki, S.O., Okagbue, H.I. and Akinlabi, G.O. Numerical solution of two-point boundary value problems via differential transform method, Global Journal of Pure and Applied Mathematics, 11 (2), pp. 801-806.
[41] Kaladhar, K. Natural Convection Flow of Couple Stress Fluid in a Vertical Channel With Hall and Joule Heating Effects, International Conference on Computational Heat and Mass Transfer-2015, Procedia Engineering, 127, 2015, pp. 1071-1078, doi: 10.1016/j.proeng.2015.11.465
[42] Jiji, L.M. Heat Convection, first ed., Springer, New York, 2006.
[43] Narahari, M. and Pendyala, R. Natural Convective Coutte Flow in a Vertical Parallel Plate Microchannel, Applied Mechanics and Materials, 705, 2015, pp. 182-187. doi:10.4028/www.scientific.net/AMM.705.182
[44] Bejan, A. Entropy Generation through Heat and Fluid Flow, Wiley, New York, 1982.

Nomenclature

B_0^2	Uniform transverse magnetic field
u, w	Velocity components in x and z directions
f, g	Dimensionless velocity
h	Channel width
f_t, f_v	Thermal and tangential momentum accommodation coefficients, respectively
ln	Fluid–wall interaction parameter
Cp	Specific heat capacity
K	Rotation parameter
Re	Reynolds number
a	Couple stress parameter
k	Coefficient of thermal conductivity
kn	Knudsen number
m	Hall current parameter
H	Hartmann number
Pr	Prandtl number
T	Temperature of fluid
T_0	Reference temperature
Pr	Prandtl number
$B\mathrm{r}$	Brinkman number
E_G	Local volumetric entropy generation rate
Be	Bejan number
Cv	Specific heats at constant volume
Ns	Dimensionless entropy generation parameter

Greek Letters

ρ	Fluid density
β_t, β_v	Dimensionless variables
γ_s	Ratio of specific heat
μ	Coefficient of viscosity
ξ	Wall-ambient temperature difference ratio
σ	Electrical conductivity
Ω	Temperature difference
η^*	Fluid particle size effect due to couple stresses
Ω^*	Angular velocity